International Journal of Industrial Ergonomics 76 (2020) 102905

Contents lists available at ScienceDirect

International Journal of Industrial Ergonomics

journal homepage: http://www.elsevier.com/locate/ergon

Single-channel SEMG using wavelet deep belief networks for upper limb motion recognition

Junkai Shao [a], Yafeng Niu [a,b], Chengqi Xue [a,*], Qun Wu [c], Xiaozhou Zhou [a], Yi Xie [b], Xiaoli Zhao [a]

[a] School of Mechanical Engineering, Southeast University, Suyuan Road, Nanjing, 211189, China
[b] Science and Technology on Electro-optic Control Laboratory, Kaixuan West Road, Luoyang, 471023, China
[c] General Design Institute, Zhejiang Sci-Tech University, Xiasha Higher Education Park, Hangzhou, 310018, China

ARTICLE INFO

Keywords:
Single-channel SEMG
Motion recognition
Singular value decomposition (SVD)
Wavelet deep belief networks (WDBN)

ABSTRACT

Surface electromyography (SEMG) has been widely used in different fields such as human machine interaction and motion recognition. A hybrid classification model based on singular value decomposition (SVD) and wavelet deep belief networks (WDBN) is firstly proposed in this paper, which allows the machine to recognize the single-joint motions of upper limb by using one channel. In this experiment, the three-joint SEMG signals of upper limb are respectively recorded through different two channels, which are employed for subsequent comparison to obtain the best single-channel of each joint. Afterwards, the collected raw signals are enhanced by SVD processing. Wavelet function is applied to replace sigmoid function as activation function for feature learning, and the spectrum signals processed by fast Fourier transform (FFT) are input to WDBN model. The results demonstrate that the recognition rates of three joint movements can be up to 100% by SVD-WDBN method, which is much better than support vector machine (SVM), back propagation (BP) neural network and extreme learning machine (ELM) model. The proposed method makes it more possible to control wearable devices with different single-channel SEMG signals, thereby the work efficiency of smart wearable devices can be improved, as well as the complexity of operations between human and machine can be reduced.

1. Introduction

Surface Electromyography (SEMG) signals can demonstrate the physiological characteristics of muscles during work with broad applications in various areas, especially in prosthetics control and EMG pattern recognition (Constantinescu et al., 2016; Liu and Wang, 2018). Since the SEMG signals in human body are weak, it is susceptible to interference and difficult to acquire. Therefore, extracting effective signal features has become the first link of SEMG signal processing (Chowdhury et al., 2013). Apparently, the accuracy of signal classification can be significantly improved by dividing complicated multi-component weak signals into many mono-component signals. Singular Value Decomposition (SVD) can effectively reduce the random noise in SEMG signals and cut down the scale of characteristic vectors (Patidar et al., 2013). Furthermore, some researchers also try to combine SVD with other algorithms, such as wavelet packet transform (WPT) (Karimi, 2012), local discriminant analysis (LDA) (Rekhi et al., 2011; Yan et al., 2019a,b), to obtain excellent recognition performance.

Currently, many studies on SEMG signal identification tend to employ multi-channel signal acquisition, which is mainly focused on different complex gestures (Geethanjali and Ray, 2011) and fine joint movements (Matrone et al., 2012), especially in the recognition of multiclass compound motions (Phinyomark et al., 2013). Meanwhile, the good recognition performance largely relies on the combination of different features and the choice of classifier. The 15 features of the SEMG time domain and respiratory amplitude were extracted, Yang et al., 2017, who effectively recognized different airway resistances of wearing respirators from SEMG and respiratory signals by artificial neural networks (ANNs). In addition, by extracting different feature sets and comparing two classifiers, Khushaba et al. (2012) successfully recognized gestures with a recognition rate of 90%. However, the above-mentioned traditional recognition methods for pattern recognition are mainly represented by shallow features, which depend on prior conditions and designed characteristics (Yan et al., 2019a,b). Its feature information still needs to be improved and its reliability needs to be further enhanced. Currently, there were only a few studies on single-channel signal recognition and the recognition accuracy was not high (Xiong et al., 2016). With the increase of channels, the

* Corresponding author.
E-mail address: ipd_xcq@seu.edu.cn (C. Xue).

https://doi.org/10.1016/j.ergon.2019.102905
Received 29 March 2019; Received in revised form 25 December 2019; Accepted 25 December 2019
Available online 3 January 2020

classification precision will be improved, but the complexity of signal processing will also be increased. In addition, more testing channels may cause inconvenient operation. These problems have greatly hindered the efficiency of recognition technology and the development of automation and intelligentization. Therefore, fewer acquisition channels are applied to obtain more effective feature representations and more stable classification models, which have become the key technique for action recognition.

In recent years, deep learning has been widely applied in the feature extraction of the SEMG signals (Chambon et al., 2018; Hinton et al., 2012). Compared with traditional learning methods, deep learning can automatically learn characteristics from big data (Chen et al., 2015). By extracting multi-level features and transferring them into the top level to form more abstract characteristic vectors that are suitable for the model classification, the accuracy of classification or prediction can be improved (Xia et al., 2018). As one of the classical models of deep learning, deep belief network (DBN) enables the underlying data to go through neural network and extracts them as high-level and meaningful feature representation (Tamilselvan and Wang, 2013; O'Connor et al., 2013). Furthermore, it can reduce overfitting and solve the intractable local minimum problem in traditional multilayer perceptron. However, it is a challenge to apply the standard restricted Boltzmann machines (RBM) directly to surface EMG pattern recognition (Chen et al., 2018). Actually, the collected SEMG signals are non-stationary and noisy during limb movements. The activation function of the standard RBM is generally selected as the sigmoid function, which is difficult to establish the accurate mapping relationship between many modes and input signals. Many current studies have proved that as a new activation function of shallow neural network, wavelet neural network (WNN) usually shows obvious advantages over traditional neural network (Yang and Hu, 2016; Khan et al., 2017). The wavelet transform can gradually multi-scale refine the SEMG signals by scaling translation, which has the characteristics of time-frequency localization. However, there are few researches on the application of wavelet method in various deep learning models. Therefore, combining the advantages of depth belief network and wavelet transform to improve the efficiency of action recognition have the vital significance.

In this paper, a hybrid classification model based on SVD-WDBN is proposed for upper limb motions - the multiclass motions with shoulder, elbow, and wrist can be identified accurately by using a corresponding single channel. The results show that the recognition rate of the SEMG signals for upper limb motions can reach 100% after classification by WDBN, which is superior to traditional methods based on SVM, BP and ELM.

2. Materials and methods

2.1. Data collection

Upper limb movements are an important activity mode in human daily life. The main purpose of this paper is to use the SEMG signals from different single channels to recognize the three joint movements of upper limb. The SEMG data can be obtained from right hands of eight healthy males. They are aged between 22 and 30 without any muscle disease. All participants must listen to the observer's instructions and pay attention to the beep of metronome. They need to complete 12 basic movements respectively. Each movement needs to be done for 5 times, each time taking 5 s. After completing a basic movement, participant should rest for 2 min to avoid muscle fatigue. The task mode loops until all experimental motions are completed.

Firstly, the 12 basic movements are categorized and given specific codes. The joint movements mainly include shoulder flexion (S1), shoulder extension (S2), shoulder abduction (S3), internal rotation (S4), external rotation (S5), elbow flexion (E1), forearm protonation (E2), forearm supination (E3), wrist flexion (W1), wrist extension (W2), ulnar deviation (W3), radial deviation (W4), which are shown in Fig. 1. Before the experiment, every participant practiced for half an hour and became familiar with all upper limb movements. Two muscles with obvious changed signals are selected from every joint of upper limb to obtain the best single-channel by experiment. (Shoulder: Ch1-Middle deltoid/Ch2-Latissimus dorsi; Elbow: Ch3-Biceps brachii/Ch4-Flexor carpi radialis; Wrist: Ch5- Flexor carpi ulnaris/Ch6- Extensor digitorum). The electrode positions of the three joints are displayed in Fig. 2.

The skin surface of muscles is cleaned with fine sandpaper and alcohol cotton balls, then the conductive electrodes are attached well to ensure a high signal-to-noise ratio (SNR). The signals of each joint movements are acquired from two muscle channels through MA300 system made by Motion Lab Systems in USA and the sampling frequency is set to 1000 Hz, while real-time raw SEMG signals are displayed in the computer.

2.2. Singular value decomposition

SVD can simplify data and eliminate noise and redundant data. In singular value decomposition, suitable feature matrices should be constructed, such as Toeplitz matrix, Cycle matrix and Hankel matrix (Jiang et al., 2015). The energy distribution of SEMG signals changes with muscle contraction, and the singular value of Hankel matrix can accurately display the component activity and energy distribution of noise in SEMG signals (Zhao and Ye, 2009). Therefore, Hankel matrix is employed to reconstruct the vector space in this article.

For a one-dimensional discrete SEMG signals disturbed by noise, $X = \{x_1, x_2, \ldots, x_L\}$, a Hankel matrix in $m \times n$ $(m \leq n)$ dimensions can be constructed.

$$H_{m\times n} = \begin{bmatrix} x_1 & x_2 & \cdots & x_n \\ x_2 & x_3 & \cdots & x_{n+1} \\ \vdots & \vdots & \vdots & \vdots \\ x_m & x_{m+1} & \cdots & x_L \end{bmatrix} \tag{1}$$

In Equation (1), H refers to a Hankel matrix and m refers to an embedding dimension, which satisfies the condition of $m + n - 1 = L$. Singular value decomposition of Hankel matrix is decomposed by singular value to obtain Eq. (2).

$$H = U\Sigma V^T \tag{2}$$

In Eq. (2), U refers to an orthogonal matrix in $m \times m$ dimensions, V refers to an orthogonal matrix in $n \times n$ dimensions, and Σ refers to a matrix in $m \times n$ dimensions.

$$\Sigma = \begin{bmatrix} \Lambda & 0 \\ 0 & 0 \end{bmatrix} \tag{3}$$

In Eq. (3), $\Lambda = diag(\lambda_1, \lambda_2, \ldots, \lambda_r)$ and $\lambda_1 \geq \lambda_2 \geq \ldots \geq \lambda_r$, where r is the rank of the Hankel matrix. The specific process of noise reduction is to set the remaining singular values to zero by keeping the first k $(k < r)$ effective singular value of the diagonal matrix. Afterwards, the reconstructed matrix can be obtained through the inverse process of singular value decomposition to obtain the denoising signals by inversion.

2.3. Wavelet deep belief network

The DBN is composed of multiple restricted Boltzmann machines (RBMs), which can automatically extract abstract features from low-level to high-level from the original data through a series of non-linear transformations. The RBM network consists of three parameters: a weight matrix $W_{n\times m}$ between the visible layer and the hidden layer, a visible node offset $b = (b_1, b_2, \ldots, b_n)$ and a hidden node offset $c = (c_1, c_2, \ldots, c_n)$. If an RBM has n visible units and m hidden units, V_m represents the state of the m-th visible unit, while H_n represents the state of the n-th hidden unit. For the state of a given set (V, H), the energy function of the RBM can be defined as

Fig. 1. Demonstration of 12 basic movements.

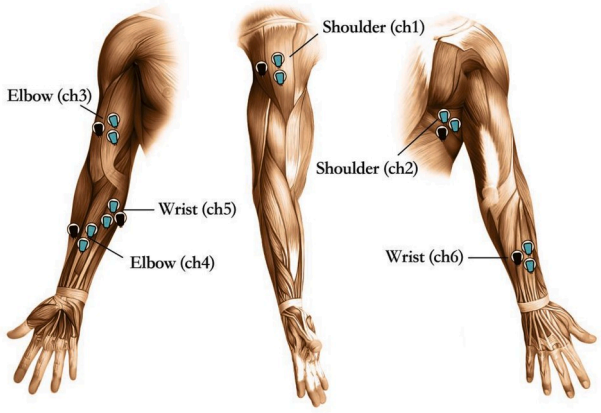

Fig. 2. Position of electrodes on the right arm.

$$E_{RBM}(V,\ H|\theta) = -\sum V_m W_{nm} H_n - \sum b_m V_m - \sum c_n H_n \tag{4}$$

In Eq. (4), θ is a parameter of RBM, which is a real number; W_{nm} represents the connection weight; b_m represents the offset of the visible layer unit m and c_n represents the offset of the visible layer unit n. Based on the energy function, the joint probability distribution of the hidden layer V and the visible layer H can be expressed as

$$P(V,\ H|\theta) = e^{-E_{RBM}(V,H|\theta)} \Big/ Z(\theta) \tag{5}$$

Set $Z(\theta)$ in Eq. (5) as a normalization factor:

$$Z(\theta) = \sum_{V,\ H} e^{-E(V,H|\theta)} \tag{6}$$

The probability distribution $P(V,\ \theta)$ of the observation data V corresponds to the edge distribution of $P(V,\ H|\theta)$, which is also regarded as a likelihood function. The edge distribution of the corresponding data is defined as

$$P(V|\theta) = \sum_h P(V,\ H|\theta) = 1 \Big/ Z(\theta) \sum_H e^{-E(V,H|\theta)} \tag{7}$$

Similarly, Eq. (8) can be obtained as

$$P(H|\theta) = \sum_V P(V,\ H|\theta) = 1 \Big/ Z(\theta) \sum_V e^{-E(V,H|\theta)} \tag{8}$$

In this paper, a new wavelet depth belief network (WDBN) is constructed by using the wavelet function instead of the traditional sigmoid function, which has a strong ability to capture the representative information of complex non-stationary vibration signal. The specific equation of the wavelet function is expressed as below

$$H_j(out) = \zeta\left(\sum_{k=1}^{m} W_{jk} x_k - d_j \Big/ c_j\right) \tag{9}$$

Where $m(i,\ k = 1, 2, \ldots, m)$ is the number of units in input layer and output layer, and the number of units in hidden layer is p ($j = 1, 2, \ldots, p$). Where ζ is the wavelet activation function, x_k is the training sample, c_j and d_j are the scale factors and shift factors of the wavelet activation function.

Wavelet transform (WT) is a new transform analysis method that inherits and develops the idea of short-time Fourier transform localization as well as overcomes the disadvantages of window Fourier transform. It is an ideal tool for time-frequency analysis and signal processing that can provide a time-frequency window that changes with frequency. In this paper, the real part of Morlet wavelet is used as a nonlinear activation function to design WDBN, which can be expressed as follows.

$$\zeta(q) = cos(5q) exp(-q^2/2) \tag{10}$$

$$H_j(out) = \zeta_{a,c}(j) = cos\left(5 \times \sum_{k=1}^{m} W_{jk} x_k - d_j \Big/ c_j\right) \times exp\left(-\frac{1}{2}\left(\sum_{k=1}^{m} W_{jk} x_k - d_j \Big/ c_j\right)^2\right) \tag{11}$$

Multiple WRBMs can form a WDBN model, as shown in Fig. 3. Each layer captures highly relevant associations from the previous hidden layer. Each low-layer WRBM serves as input data for training the next WRBM, which circulates as many layers as possible, and further enhances the feature extraction capability of the network by fine-tuning the given parameters.

2.4. SVD-WDBN classification method

SVD has good stability and invariability for non-linear and non-stationary weak signal processing (Lehtola et al., 2008). It can extract the feature information of the SEMG to the greatest extent, as well as reconstruct and enhance the signal features. The entire identification flow chart is shown in Fig. 4. Firstly, the SVD noise reduction technique is applied to enhance the original SEMG signals and then the enhanced signals are further processed into the frequency domain signals by FFT. Finally, WDBN is applied to extract high-level features layer by layer from the processed signals to achieve effective classification.

In this paper, the advantages of the SVD signal enhancement and the WDBN intelligent classification are organically combined to form a new method to identify the SEMG signals of upper limb movements. This method is mainly divided into two stages:

Weak signal enhancement stage:

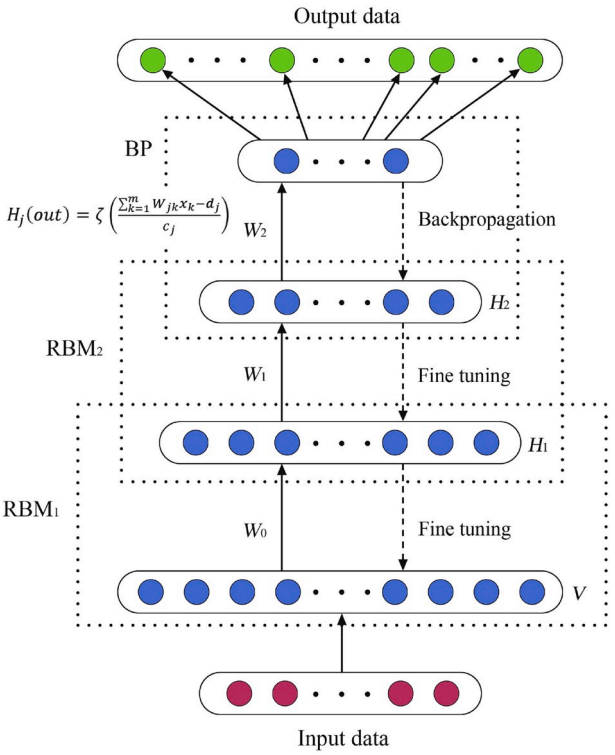

Fig. 3. Principle structure diagram of WDBN.

Step1: Obtain the SEMG signals;
Step2: Initialize SVD parameters;
Step3: Decompose and reconstruct the early weak signals to obtain the enhanced signals;
Step4: Convert the normalized signals into the spectrum signals by FFT, then divide those signals into the training samples and the test samples.

Intelligent identification stage:

Step5: Perform wavelet function as the activation function, initialize the WDBN model parameters;
Step6: Use the unlabeled samples to train the WDBN model, determine the number of hidden layers (N) through unsupervised CD manner in each layer;
Step7: Slightly adjust the model parameters and save the network structure according to the sample label;
Step8: Obtain the WDBN model, test and classify the test samples and generate the classification result.

3. Results and discussion

This paper focuses on the single-channel SEMG signal identification of upper limb movements, which has practical application significance for controlling humanoid machinery and prosthetics.

In the first experiment, the SEMG signals are enhanced by SVD, the effects of time domain and frequency domain before and after SVD noise reduction are compared. In the second experiment, the original signals and denoising signals collected from different channels are classified by WDBN, the clustering and classification characteristics of data distribution are analyzed, and the recognition accuracy under two processing methods are compared. Finally, the best single-channel of each joint for SEMG recognition is determined. The third experiment is based on the optimal single-channel signals of each joint, the recognition effects of WDBN are compared with other classification methods.

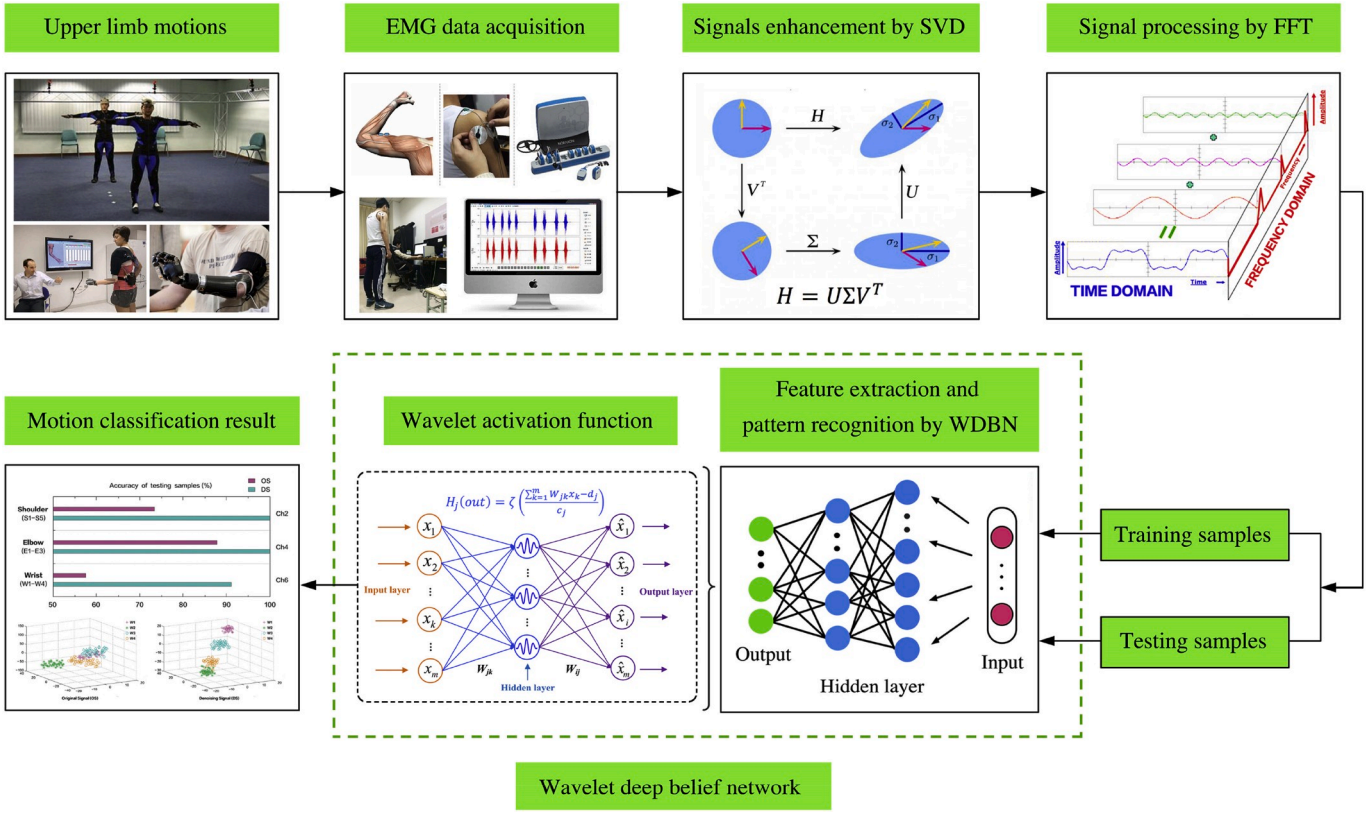

Fig. 4. The entire identification flow diagram.

3.1. Evaluate the performance of SVD

The SEMG signals are very weak and susceptible to influences of the external environment and internal factors, which make it more difficult to extract the valid features. Therefore, signal denoising has always been a very important step in signal processing. In order to evaluate the performance of SVD in signal decomposition and feature extraction, the waveform characteristics of SEMG signals are analyzed in time and frequency domain, and the spectrum signals are obtained by the FFT-based method. Due to limited display space, only the original signals (OS) and denoising signals (DS) of three movements on Ch1 are shown in Figs. 5 and 6.

The time-domain waveforms of three SEMG signals before and after noise reduction are shown in Fig. 5. It can be seen that different upper limb movements have different characteristic frequencies, and their waveforms are very distinct. In the time domain waveform, a great amount of noise is removed. After SVD noise reduction for the SEMG signals of S1, S2, and S3, some important characteristics of the signals are largely retained.

The waveforms of the spectrum signals before noise reduction are relatively messy, and the impact components are not obvious in Fig. 6. However, the spectral characteristic frequencies of the three motions after noise reduction become more prominent. Similarly, it makes sense that the energy impact components all appear between 30 Hz and 50 Hz. This is because the interference and cross components in the original signals are separated, while the larger characteristic components of the signals can be retained.

Generally, the time-frequency analysis of the traditional signals cannot quantify the characteristic information of upper limb movements and the description ability is limited. However, SVD can effectively strengthen the weak components of the signals and suppress the background noise. In this paper, the spectrum signal processed by FFT are selected as the input signals.

3.2. Recognition accuracy of WDBN

In this section, based on the SVD denoising signals and unprocessed raw signals, a new WDBN model is constructed by using wavelet function as the activation function, which is firstly employed to identify the 12 kinds of upper limb movements. Each movement uses 5,000 sampling points as a sample group. A total of 200 ($8 \times 5 \times 5$) shoulder samples are constructed for 8 subjects. The number of elbow samples is 120 ($8 \times 5 \times 3$) and the number of wrist samples is 160 ($8 \times 5 \times 4$), 50% of which are used as training samples and the other 50% as test samples. The WDBN parameters are set to the double-tier RBMs characteristic layer, and the neural network is set to 5000-100-100-12. Given the stability and convergence speed of the algorithm, the learning rate ε and α in the backward fine-tuning both take a common value of 0.1. The initial number of iterations is set to 100. The Test is repeated 20 times, and the average value is regarded as the final recognition result.

The effect of model training mainly depends on the recognition rate of the given test samples, in other words, how many test samples can be identified by the trained WDBN model. In this section, the WDBN model is used to identify two signal sources, including the original signals (OS) and denoising signals (DS), and the classification results of the test data set are obtained finally. In order to compare the differences between these two classification results more intuitively, we show the recognition rates of three motion test samples on Ch2/Ch4/Ch6.

By comparing the test sample results in Fig. 7, it can be found that for the original signals that have been classified by WDBN, the overall recognition effect is not high. After noise reduction, the classification results of the three joints are significantly improved. In particular, the recognition accuracy of shoulder and elbow movements can reach to 100%. This shows that the redundant information of the SEMG signals is eliminated after SVD noise reduction, and the classification performance of WDBN is effectively enhanced. It is noteworthy that in the signal classification after noise reduction, the test data samples for some wrist movements are still not identified.

The more detailed classification of 80 test samples on the wrist are shown in Fig. 8. It can be seen that some test data points in the original signals have not been accurately classified. On the one hand, due to the relatively low SNR of original signals and the interference of background noise, these lead too much useless information and hinder the training recognition of the classifier. On the other hand, there may be some differences between the SEMG mode and the fineness of joint movements. Firstly, human shoulder and elbow movements belong to a wide range of joint motions. Therefore, the energy features of the signals generated by muscles are more abundant, which is conducive to the precise classification of the model. Secondly, the collecting area of wrist muscle is comparatively small and are susceptible to interference from

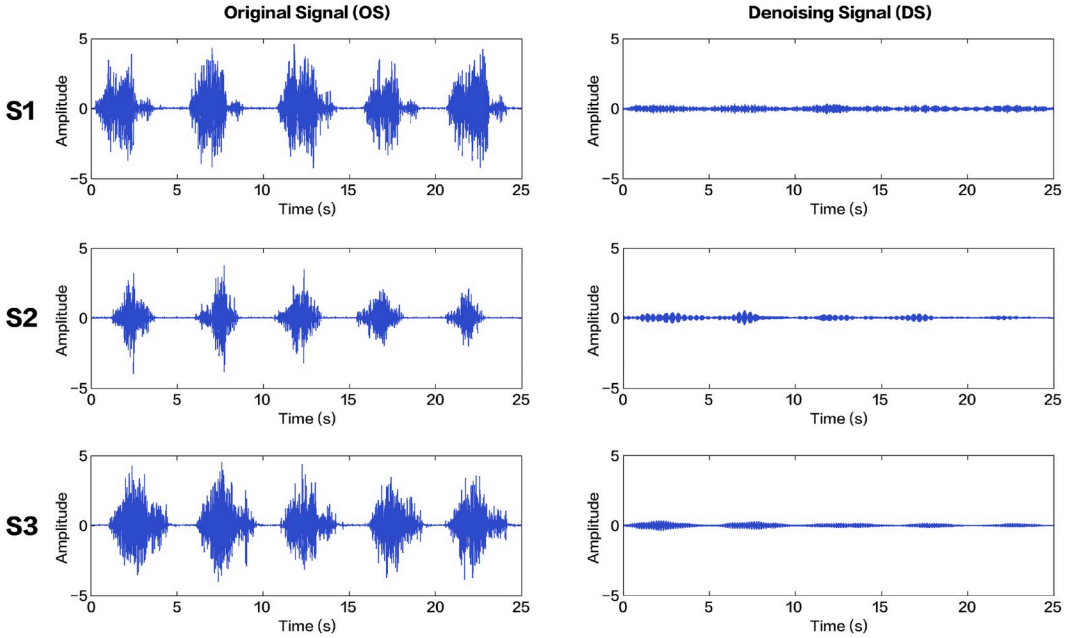

Fig. 5. The time-domain waveform before and after noise reduction (S1/S2/S3).

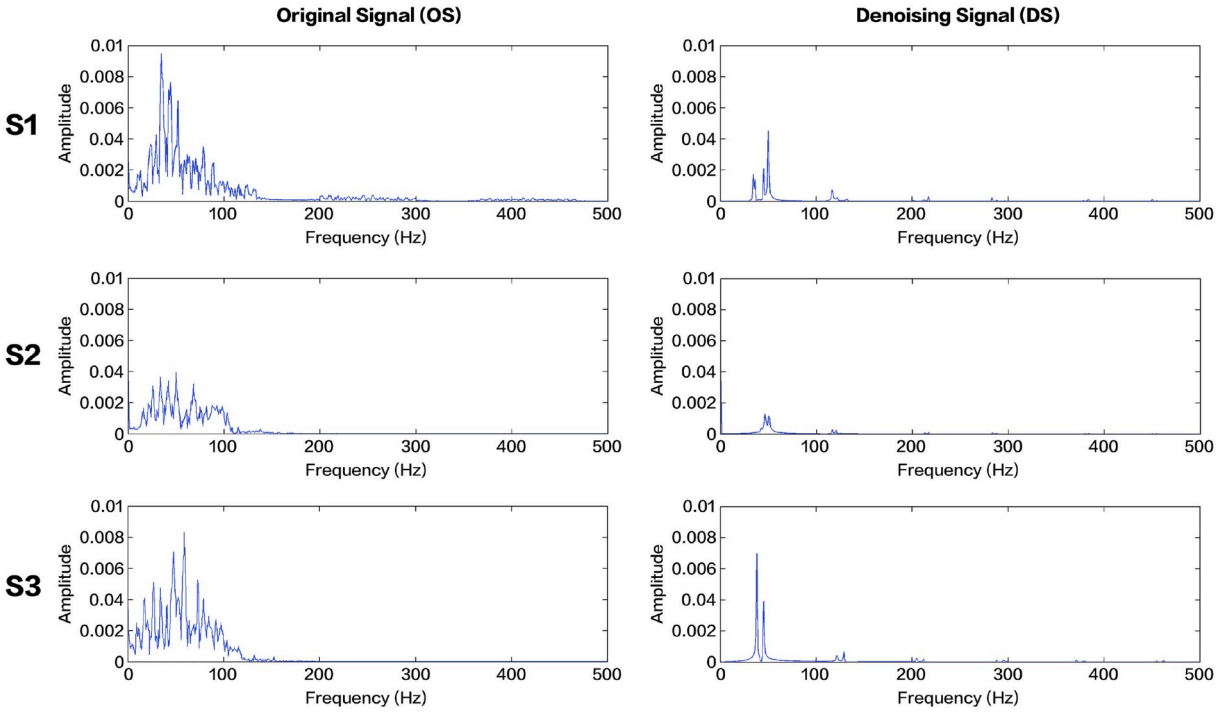

Fig. 6. The spectrum diagram before and after noise reduction (S1/S2/S3).

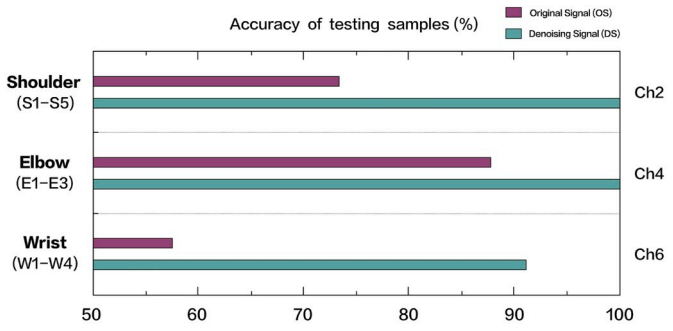

Fig. 7. The test sample identification rates before and after noise reduction.

adjacent muscle groups, and the muscles selected from the shoulder and elbow joints belong to the large muscle groups, which can provide more reliable and comprehensive data features. Thus, the classification effect of shoulder and elbow motions can reach to 100%.

Two classification results before and after signal enhancement are effectively visualized by t-distributed stochastic neighbor embedding (t-SNE), which is beneficial for us to analyze the data distribution more intuitively. In this section, in order to accelerate the calculation of pairwise preferences between different dimensional points and suppress some noise without seriously distorting the distance between the points. The principal component analysis (PCA) algorithm is used to reduce the dimensionality of the feature data to 50, while the t-SNE algorithm is used to convert 50-dimensional representation to a 3-dimensional map. Figs. 9–11 show the distribution of total samples from eight subjects:

The above three figures show that the data distributions for the 12 types of motions identified by the original signals have different degrees of intersection and fusion. The overall samples of the three joint motions are loosely distributed and the clustering effect is poor. For example, among the five movements of shoulder, only S2 and S4 show a good separation effect, and the other three movements are all overlapped, so it is difficult to accurately classify them. However, the data points of

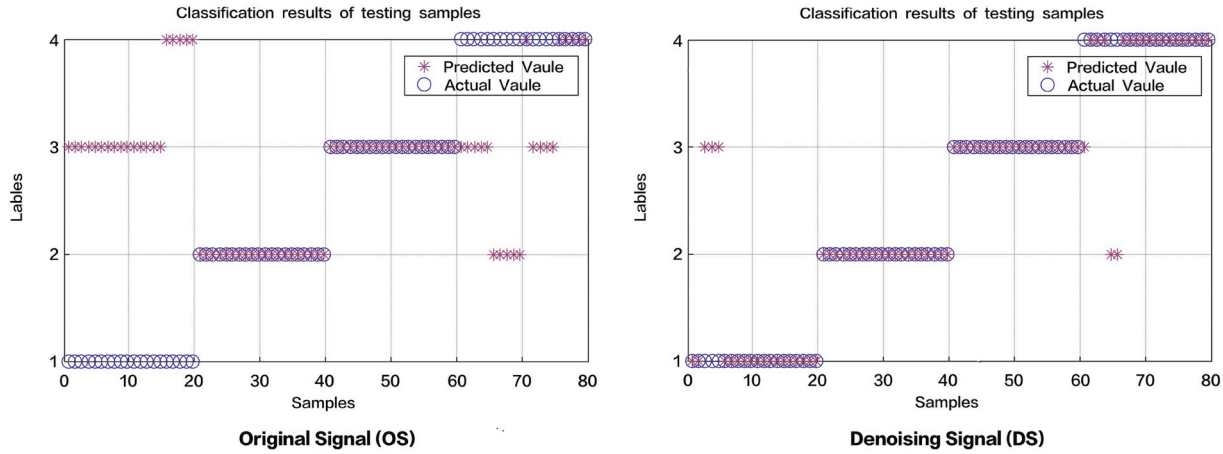

Fig. 8. Classification of test samples for wrist motions (W1–W4).

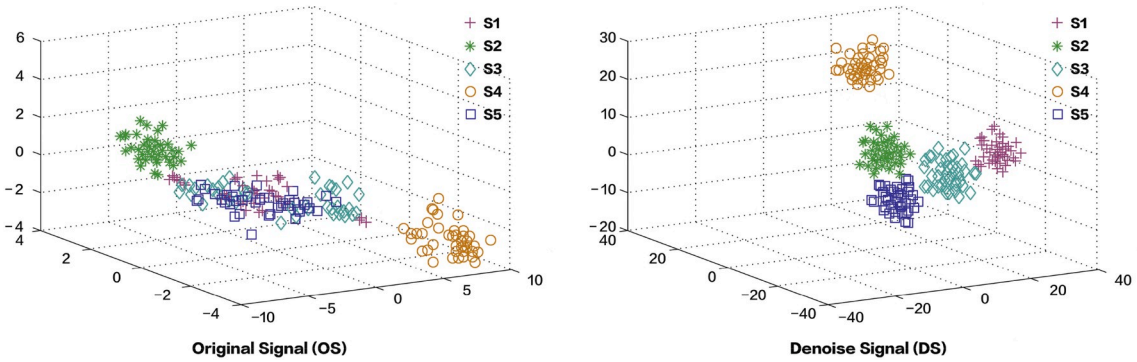

Fig. 9. Distribution of total samples for shoulder movements (S1–S5).

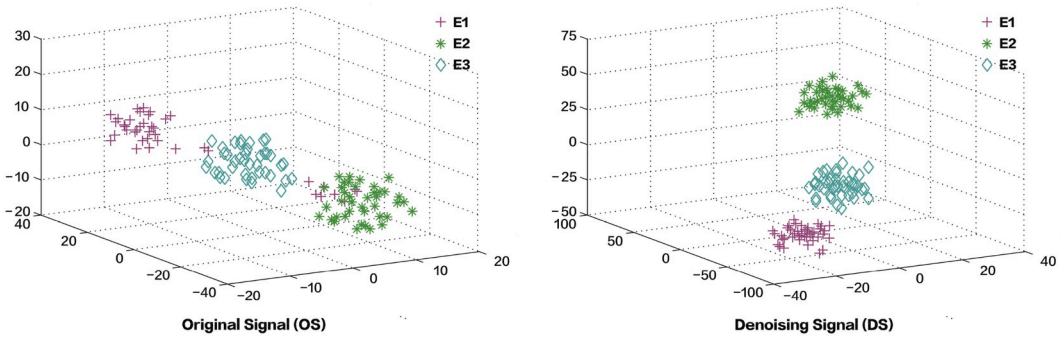

Fig. 10. Distribution of total samples for elbow movements (E1-E3).

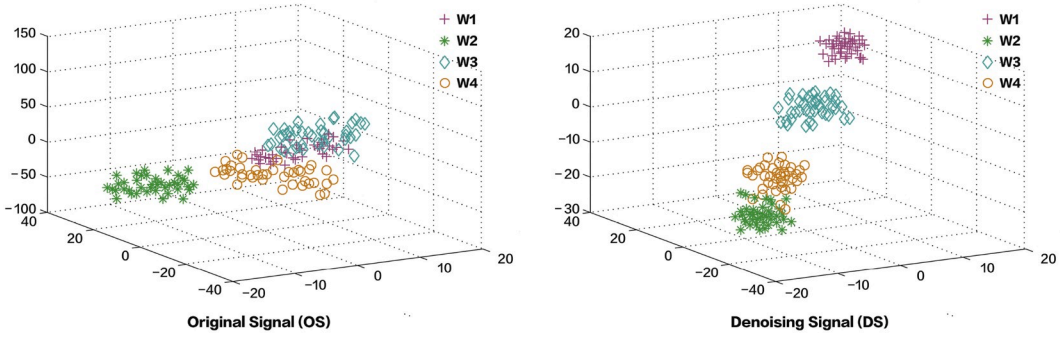

Fig. 11. Distribution of total samples for wrist movements (W1–W4).

shoulder, elbow and wrist motions identified by the denoising signals concurrently show the distribution characteristic of small intra-class distance and large inter-class spacing. The extracted features have good separability and can be used to classify the 12 types of movements. This proves that after enhancing the signals through SVD, the clustering and classification of three-dimensional features of data samples are the best.

3.3. Selection of optimal channel

The correct selection of the SEMG channel that can be used to identify upper limb motions is very important, because it can improve the classification accuracy of different models. Table 1 shows the channel recognition rates of the three joints, including training samples and test samples. It can be seen that the overall recognition rate after signal enhancement is much better than the unenhanced recognition rate. This shows that the SEMG signals processed by SVD improves the classification ability and generalization performance of WDBN. Compared with the WDBN classification method based on the original signals, it has obvious advantages. This is because SVD can reduce the interference components of the SEMG signals, eliminate redundancy and facilitate the feature learning and classification of WDBN at a later period.

As can be seen from Table 1, each joint has an optimal single-channel with a recognition rate of 100%. The best channel for shoulder action recognition is Ch2. The two channels of elbow movements have the best performance, while the best channel of wrist movements is Ch5. Because the SEMG acquisition process can be easily interfered by many factors,

Table 1
Channel recognition rates of three joints.

Input signals	Ch1 (S1–S5)	Ch2 (S1–S5)	Ch3 (E1-E3)	Ch4 (E1-E3)	Ch5 (W1–W4)	Ch6 (W1–W4)
OS	0.8	0.76	0.917	0.917	0.725	0.613
DS	0.95	1	1	1	1	0.938

some errors in the recognition rate are acceptable.

3.4. Comparison with different classifiers

For a long time, SVM or BP-based classifiers have become a popular method and improved classification accuracy. In addition, the application of ELM has also made great progress in the field of SEMG signal recognition (Wu et al., 2017; Cao et al., 2015). In the previous sections, the weak signals can be effectively enhanced by SVD, the good results of noise reduction are achieved, and the best recognized channels are determined.

In this section, based on the optimal single-channel of each joint, the averages of upper limb motion recognition are obtained by using WDBN and other classifiers under different conditions. SEMG signals are easily affected by many random interferences, including current interference, physical quality or experimental environment. In order to verify the anti-noise capability of SVD-WDBN, when other parameters are unchanged, such as the ratio of training samples and testing samples, the raw data is mixed with the interference coefficients a ($a = 0.2$, 0.4, 0.6 and 0.8 rand noise are added to the experimental data set, respectively). Therefore, the data set x is changed into $X_{new} = x + a.\text{rand}(\text{size}(x))$, where size($x$) represents the signal size and the rand (*) function is a random function that generates random numbers in MATLAB.

Meanwhile, the time-domain feature set is built, 16 commonly used time domain statistical characteristic parameters are showed in Table 2. The original electromyography is converted into a statistical feature data set. In this study, the traditional artificial feature parameters are defined as AF.

From Table 3, it can be seen that under different interference coefficients, compared with classification results of traditional artificial feature parameters by SVM, BP and ELM, AF-WDBN has the best classification effect, and the average accuracy of all samples can achieve 100%. However, when the interference coefficient is 0.4, the recognition accuracy of SVD-WDBN can still reach 100%. This suggests that the proposed SVD-WDBN hybrid recognition model has strong classification ability as well as good anti-noise performance. In general, the recognition accuracy of the above-mentioned four classification methods decreases as the interference coefficient increases. When the interference coefficient of the SEMG signals is increased to 0.8, the results of SVM, BP and ELM classifiers are lower than 65%, but the recognition accuracy of SVD-WDBN remains at about 95%. It is worth noting that the falling gap in SVD-WDBN classification accuracy is only 0.058 when the interference coefficient is set to 0.2 and 0.8. In comparison, the recognition accuracy of the other three classifiers has a floating gap between 0.2 and 0.3. This shows that the range of WDBN is the smallest within the overall reduction range. Deep learning can realize the approximation of complex function, represent the characterization distribution of the input data and demonstrate the great ability to learn the essential characteristics of data sets from a small number of samples. In this study, the stability and generalization ability of SVD-WDBN is proven to be the best, which is suitable for single-channel automated identification of upper limb SEMG signals.

In this paper, the exploration of motion recognition model is limited to the classification of the basic movements of the three joints, while human upper limb movements are coherent and complex, so future work will focus on identifying the spatial coherent motions of upper limb and increasing the sample database. At the same time, the combination of data flow segmentation and moving window will enhance the consistency of action recognition in the system and avoid the delay effect of different peripheral devices. On the other hand, the adjustment of hyperparameters for deep learning has always been a problem. How to ensure that the trained model parameters have good generalization, which has great positive significance for practical engineering applications. Therefore, we will explore the parameter optimization and regularization technique of the model in the future to prevent the model from overfitting.

Table 2
Time domain statistical characteristic parameters.

Number	Feature Parameter	Number	Feature Parameter
1	Mean Value	9	Kurtosis
2	Mean Square Amplitude	10	Standard Deviation
3	Square Root of Amplitude	11	Waveform Index
4	Average Amplitude	12	Peak Index
5	Maximum Value	13	Impulsion Index
6	Minimum Value	14	Tolerance Index
7	Peak to Peak	15	Slope Index
8	Skewness	16	Kurtosis Index

Table 3
The averages of different classification methods.

Interference Coefficient	$g = 0.2$	$g = 0.4$	$g = 0.6$	$g = 0.8$	Average
AF-SVM	0.85	0.75	0.7	0.65	0.738
AF-ELM	0.9	0.813	0.708	0.6	0.755
AF-BP	0.833	0.75	0.667	0.563	0.703
AF-WDBN	1	0.967	0.917	0.85	0.934
SVD-WDBN	1	1	0.967	0.942	0.977

3.5. Experimental verification of the proposed model and database

In human motion recognition, gestures are a complex and delicate motions, so gesture recognition puts forward higher requirements for model performance. Therefore, in order to verify the effectiveness of the proposed method, we select EMG data of four gestures collected through 8 channels, which are obtained from Kirill (2018) in Kaggle. The four gestures consist of rock, scissors, paper and ok. Each gesture is recorded 6 times at 200HZ for 20s. Each gesture stays in a fixed position for 120s. In this section, we randomly selected four channels (Ch1/Ch3/Ch5/Ch7) for recognition. The sliding window is used to process signals to form data samples for the whole experiment. The moving window size is 50, and the length of time is 200. A total of 40 data samples are obtained for each gesture. Here, we refer to the data processing method of the previous sections. Due to limited space, we randomly select gesture 3 data based on Ch1 to display the time domain waveform and frequency spectrum before and after SVD noise reduction in Fig. 12.

After SVD processing, both time domain waveform and frequency spectrum in Fig. 12 show good performance. Especially from the spectrogram, we can see that the signal characteristics have been strengthened. The energy impact components appear between 40 Hz and 50 Hz, which provides a basis for improving the model recognition rate.

A gesture is performed by many small muscle groups, and different muscle channels show different recognition effects. This is because some muscles belong to cooperative movement and some muscles belong to active movement, and not every muscle channel plays a major role in completing a complex movement. As can be seen from all the recognition rates of four channels in Table 4, the classification effects of the denoising signals are obviously higher than the original signals. However, the best recognition rate after noise reduction is only 87.5%, and there are still some motions that have not been accurately identified yet. The reason for this may be that gestures belong to fine movements, the synergy between hand muscles is relatively high, and the vibration energy generated by small muscle groups is easy to overlap, so it is difficult to recognize multiple gestures from a single channel. In addition, the open data has a sampling rate of only 200 HZ, which may not capture all the valid features of the original signals.

The more detailed classification of test samples for four gestures on Ch1 are shown in Fig. 13. It can be seen that the recognition rate of gesture1 (Rock) can reach 100% after denoising, but gesture3 (Paper) is still the worst. It may be due to the muscle vibration energy produced by the stretching movement of the hand is lower than that by the

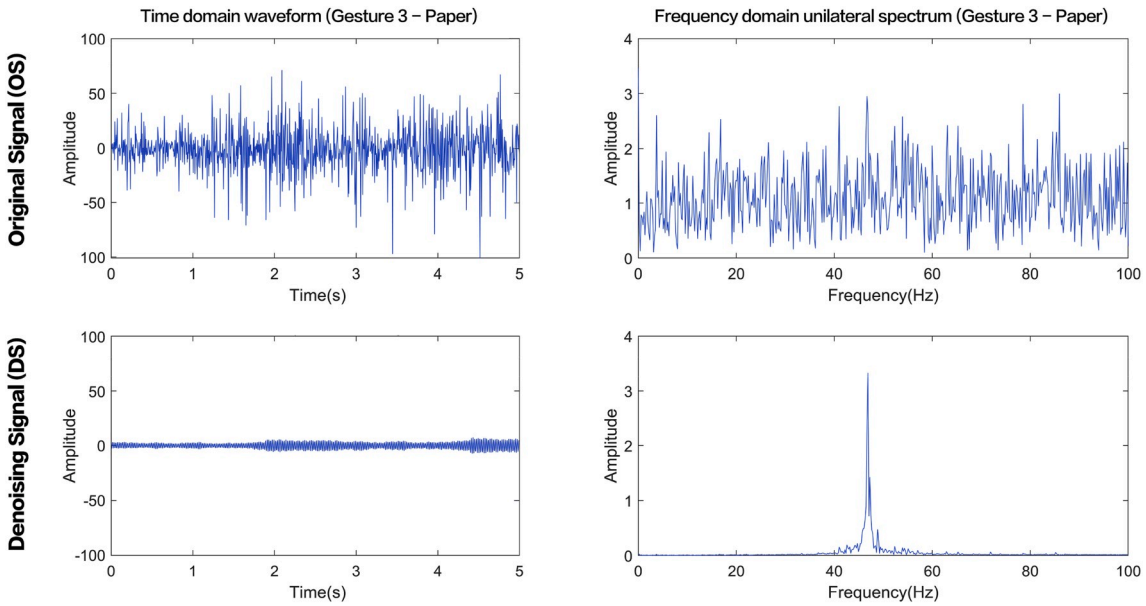

Fig. 12. The time domain waveform and frequency spectrum on Ch1 (Gesture 3-Paper).

Table 4
The recognition rates of test samples for four gestures.

Input signals	Ch1	Ch3	Ch5	Ch7
OS	0.613	0.763	0.588	0.725
DS	0.775	0.875	0.75	0.838

contraction movement, which is not conducive to recognition. Nevertheless, the recognition of four delicate gestures by using a single channel based SVD-WDBN model can approach 90%. The results basically verify the effectiveness of the proposed method. We believe that by increasing the data sampling rate, selecting the appropriate muscle channels, and re-optimizing the model, the single channel recognition can achieve more satisfactory effects for gestures.

4. Conclusions

In this paper, the SEMG signals of each joint are collected through two channels. After the original signals are processed by SVD noise reduction, the FFT-processed spectrum signals are input to the WDBN model. The best single channel of each joint is determined by comparing the recognition of two channels. Based on the best single-channel data collected by three joints, the total recognition rates of WDBN and other classifiers are compared. The results show that SVD-WDBN method no longer relies on artificial feature extraction, which is more effective than traditional methods and standard deep learning methods. In this paper, the singular value decomposition, wavelet function and deep belief network are creatively combined to further expand the research of single-channel SEMG signal recognition method.

Informed consent

Informed consent was obtained from all individual participants included in the study.

Ethical approval

There are no requirements for ethical approval.

Declaration of competing interest

The authors declare that they have no conflict of interest.

CRediT authorship contribution statement

Junkai Shao: Methodology, Software, Formal analysis, Writing - original draft. **Yafeng Niu:** Methodology, Investigation, Writing -

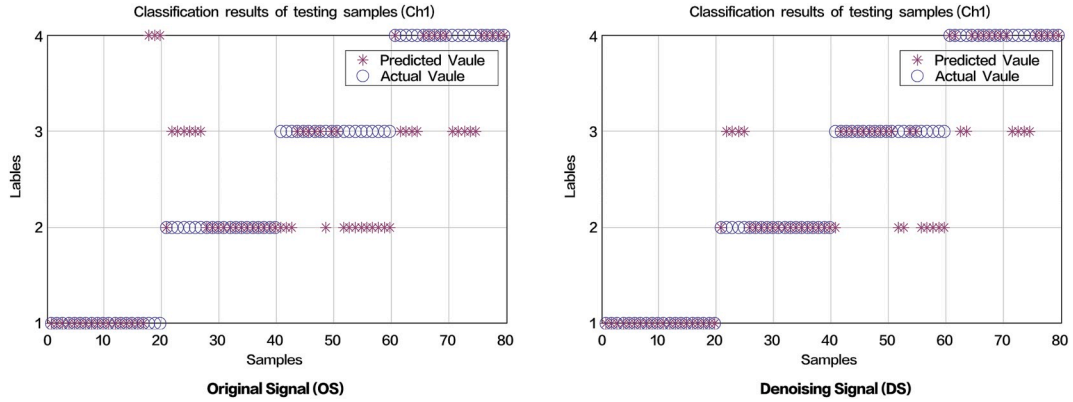

Fig. 13. Classification of test samples for four gestures on Ch1.

review & editing. **Chengqi Xue:** Conceptualization, Supervision, Funding acquisition. **Qun Wu:** Conceptualization, Methodology. **Xiaozhou Zhou:** Visualization, Data curation. **Yi Xie:** Funding acquisition, Project administration. **Xiaoli Zhao:** Software, Validation.

Acknowledgments

The authors would like to gratefully acknowledge the reviewers' comments. This work was supported jointly by National Natural Science Foundation of China (No. 71871056, 71801037, 71901061), Postgraduate Research & Practice Innovation Program of Jiangsu Province (No. SJKY19_0067), Science and Technology on Avionics Integration Laboratory and Aeronautical Science Fund (No. 20165169017, 20185569008), SAST Foundation of China (SAST No. 2016010), Equipment Pre research & Ministry of education of China Joint fund, Fundamental Research Funds for the Central Universities of China (No. 2242019k1G023).

Appendix A. Supplementary data

Supplementary data to this article can be found online at https://doi.org/10.1016/j.ergon.2019.102905.

References

Cao, H., Sun, S., Zhang, K., 2015. Modified EMG-based handgrip force prediction using extreme learning machine. Soft Comput 21 (2), 1–10.
Chambon, S., Galtier, M.N., Arnal, P.J., Wainrib, G., Gramfort, A., 2018. A deep learning architecture for temporal sleep stage classification using multivariate and multimodal time series. IEEE Trans. Neural Syst. Rehabil. Eng. 26 (4), 758–769.
Chen, Y., Zhao, X., Jia, X., 2015. Spectral-spatial classification of hyperspectral data based on deep belief network. IEEE J. Sel. Top. Appl. Earth Obs. Remote Sens. 8 (6), 2381–2392.
Chen, J., Zhang, X., Cheng, Y., Xi, N., 2018. Surface EMG based continuous estimation of human lower limb joint angles by using deep belief networks. Biomed. Signal Process. Control 40, 335–342.
Chowdhury, R.H., Reaz, M.B.I., Ali, M.A.B.M., Bakar, A.A.A., Chellappan, K., Chang, T. G., 2013. Surface electromyography signal processing and classification techniques. Sensors 13 (9), 12431–12466.
Constantinescu, G., Jeong, J.W., Li, X., Scott, D.K., Jang, K.I., Chung, H.J., et al., 2016. Epidermal electronics for electromyography: an application to swallowing therapy. Med. Eng. Phys. 38 (8), 807–812.
Geethanjali, P., Ray, K.K., 2011. Identification of motion from multi-channel EMG signals for control of prosthetic hand. Australas. Phys. Eng. Sci. Med. 34 (3), 419–427.
Hinton, G., Deng, L., Dong, Y., George, E.D., Abdel, R.M., Navdeep, J., 2012. Deep neural networks for acoustic modeling in speech recognition: the shared views of four research groups. IEEE Signal Process. Mag. 29 (6), 82–97.
Jiang, H., Chen, J., Dong, G., Liu, T., Chen, G., 2015. Study on Hankel matrix-based SVD and its application in rolling element bearing fault diagnosis. Mech. Syst. Signal Process. 52–53 (1), 338–359.
Karimi, M., 2012. Forearm EMG signal classification based on singular value decomposition and wavelet packet transform features. Adv. Mater. Res. 433–440 (2), 912–916.
Khan, M.M., Mendes, P., Zhang, p., Chalup, S.K., 2017. Evolving multi-dimensional wavelet neural networks for classification using Cartesian genetic programming. Neurocomputing 247, 39–58.
Khushaba, R.N., Kodagoda, S., Takruri, M., Dissanayake, G., 2012. Toward improved control of prosthetic fingers using surface electromyogram (EMG) signals. Expert Syst. Appl. 39 (12), 10731–10738.
Kirill, Y., 2018. Classify Gestures by Reading Muscle Activity. https://www.kaggle.com/kyr7plus/emg-4.
Lehtola, L., Karsikas, M., Koskinen, M., Huikuri, H., Seppanen, T., 2008. Effects of noise and filter on SVD-based morphological parameters of the T wave in the ECG. J. Med. Eng. Technol. 32 (5), 400–407.
Liu, H.Y., Wang, L.H., 2018. Gesture recognition for human-robot collaboration: a review. Int. J. Ind. Ergon. 68, 355–367.
Matrone, G., Cipriani, C., Carrozza, M., Magenes, G., 2012. Real-time myoelectric control of a multi-fingered hand prosthesis using principal components analysis. J. NeuroEng. Rehabil. 9 (1), 40–52.
O'Connor, P., Neil, D., Liu, S.C., Delbruck, T., Pfeiffer, M., 2013. Real-time classification and sensor fusion with a spiking deep belief network. Front. Neurosci. 7 (7), 1–13.
Patidar, M., Jain, N., Agrawal, P., 2013. EMG signals classification based on singular value decomposition and neural network. Int. J. Sci. Eng. Res. 4 (6), 956–960.
Phinyomark, A., Quaine, F., Charbonnier, S., Serviere, C., Bernard, F.T., Laurillau, Y., 2013. EMG feature evaluation for improving myoelectric pattern recognition robustness. Expert Syst. Appl. 40 (12), 4832–4840.
Rekhi, N.S., Arora, A.S., Singh, H., 2011. Comparison of local discriminant analysis and singular value decomposition for classification of surface EMG signal. Acad. Res. Int. 1 (2), 84–88.
Tamilselvan, P., Wang, P., 2013. Failure diagnosis using deep belief learning based health state classification. Reliab. Eng. Syst. Saf. 115 (7), 124–135.
Wu, Q., Shao, J.K., Wu, X.H., Zhou, Y.J., Liu, F.P., Xiao, F., 2017. Upper limb motion recognition based on LLE-ELM method of sEMG. Int. J. Pattern Recognit. Artif. Intell. 31 (6), 1–16.
Xia, P., Hu, J., Peng, Y., 2018. EMG-based estimation of limb movement using deep learning with recurrent convolutional neural networks. Artif. Organs 42 (5), 67–77.
Xiong, A., Ding, Q., Zhao, X., Han, J., Liu, G., 2016. Classification of hand gestures based on single-channel sEMG decomposition. J. Mech. Eng. 52 (7), 175–179.
Yan, X., Liu, Y., Jia, M., et al., 2019a. A multi-stage hybrid fault diagnosis approach for rolling element bearing under various working conditions. IEEE Access 7, 138426–138441.
Yan, X., Liu, Y., Jia, M., 2019b. Health condition identification for rolling bearing using a multi-domain indicator-based optimized stacked denoising autoencoder. Struct. Health Monit. 1475921719893594.
Yang, H.J., Hu, X., 2016. Wavelet neural network with improved genetic algorithm for traffic flow time series prediction. Optik-International Journal for Light and Electron Optics 127 (19), 8103–8110.
Yang, Z.L., Chen, Y.M., Wang, J.P., Gong, H., 2017. Recognizing the breathing resistances of wearing respirators from respiratory and sEMG signals with artificial neural networks. Int. J. Ind. Ergon. 58, 47–54.
Zhao, X., Ye, B., 2009. Similarity of signal processing effect between Hankel matrix-based SVD and wavelet transform and its mechanism analysis. Mech. Syst. Signal Process. 23 (4), 1062–1075.